

Electronic Structure of 4,6-bis{5-amino-3-*tert*-butyl-4-[(3-methyl-1,2,4-thiadiazol-5-yl)diazeneyl]-1*H*-pyrazol-1-yl}-1,3,5-triazin-2(1*H*)-one of the *trans* Form Used for Yellow Ink Jet Inks

Hiroki Shibata and Jin Mizuguchi[▲]

Department of Applied Physics, Yokohama National University, Yokohama 240-8501, Japan

E-mail: mizu-j@ynu.ac.jp

Abstract. The authors have been interested in a sodium-containing bisazo complex of the *cis* form for application as a yellow ink jet ink pigment. It exhibits good performance with respect to light and heat stability but is rather poor with respect to solvent fastness. Accordingly, an attempt has been made in the present investigation to improve the solvent fastness by eliminating the sodium atom from the Na complex to give a structurally more stable bisazo compound of the *trans* form (i.e., the title compound). Treatment of the complex with hydrochloric acid removed the sodium atom and also transformed the product from the *cis* to the *trans* form, shown by the structural analysis as reported in the companion article. In this article, the authors report electronic characterization which was carried out computationally and experimentally. The absorption maximum in solution appears at about 450 nm and is composed of two electronic transitions with the following configuration interaction (CI) components: (i) HOMO–1 → LUMO and HOMO → LUMO+1 and (ii) HOMO → LUMO+1, HOMO → LUMO+2, and HOMO–1 → LUMO, where the HOMO, LUMO, and CI stand for the highest occupied or the lowest unoccupied molecular orbitals and the configuration interaction, respectively. The title compound possesses high solvent fastness in addition to the light and heat stability of the original compound. © 2011 Society for Imaging Science and Technology. [DOI: 10.2352/J.ImagingSci.Technol.2011.55.2.020505]

INTRODUCTION

As is well known, azo pigments are widely used in imaging and printing industries because of their versatile colors, high tinctorial strength, as well as their low price.¹ However, the azo pigments are generally inferior in light, heat, and solvent fastness to phthalocyanines (blue), peryleneimides (vivid red via maroon to black), quinacridones (red and magenta), pyrrolopyrroles (red), although considerable effort has been directed to improve these properties. Under these circumstances, we came across a novel bisazo compound of 2,6-bis[5-amino-3-*tert*-butyl-4-(3-methyl-1,2,4-thiadiazol-5-yl)diazeneyl]-1*H*-pyrazol-1-yl]-1,3,5-triazin-4(1*H*)-one of the *cis* form published by Nagata and Tateishi.² [B-PAT: Figure 1(a), whereas Fig. 1(b) shows the *trans* form: the title compound.] We tackled this compound and found that it exhibits a good performance in light and heat stability but

rather poor in solvent fastness. Then, we tried to remove its drawback from the standpoint of the crystal structure by growing single crystals for structure analysis. Unexpectedly, we have isolated three kinds of single crystals from the reaction product of B-PAT: two bisazo^{3,4} and one monoazo⁵ compounds. This indicates that the product was not a pure material but a mixture of monoazo and bisazo compounds. To our even greater surprise, the bisazo compounds are found to include sodium atoms in the form of five-coordinate Na complexes in a *cis* fashion [Na-containing B-PAT:^{3,4} about 80% of the product; Figure 2(a)]. On the other hand, the monoazo compound is Na-free M-PAT⁵ [about 20%; Fig. 2(b)]. Then, an attempt has been made to improve the solvent fastness by eliminating the sodium atom from the Na complex to give a structurally more stable bisazo compound of the *trans* form (i.e., the title compound: B-PAT of the *trans* form). As expected, we were able to isolate the target compound using hydrochloric acid (HCl) as

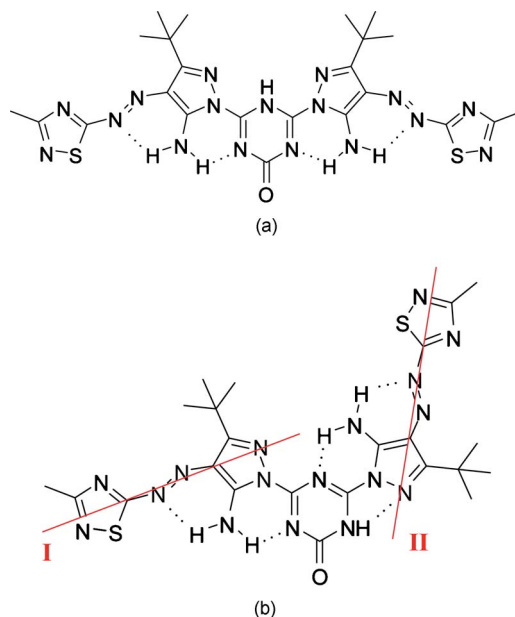


Figure 1. Structure of B-PAT: (a) *cis* form and (b) *trans* form. The solid lines in Fig. 1(b) designate the directions of the transition dipole as calculated from the molecular orbital calculations.

[▲]IS&T Member.

Received Aug. 12, 2010; accepted for publication Jan. 8, 2011; published online Mar. 10, 2011.

1062-3701/2011/55(2)/020505/6/\$20.00.

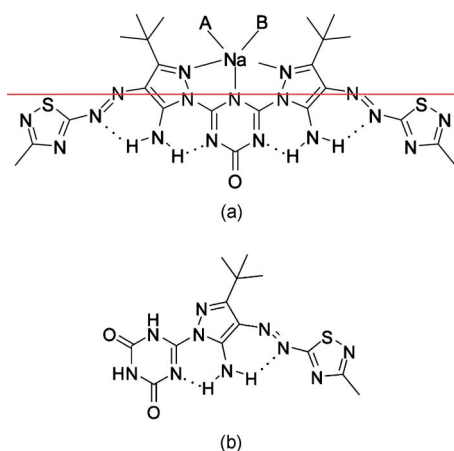


Figure 2. Structure of three isolated crystals: (a) Na-containing B-PATs of the *cis* form (B-PAT I with A=methanol and B=phenol; B-PAT II with A=water and B=NMP) and (b) Na-free M-PAT. The red line denotes the direction of the transition dipole as calculated from molecular orbital calculations. (The presence of the sodium atom has no effect on the direction of the transition dipole.)

the eliminating agent.⁶ The structure of the above four different crystals (Na-containing B-PAT I and II of the *cis* form, Na-free M-PAT, and Na-free B-PAT of the *trans* form) has been analyzed and presented in our previous paper.⁷

In the present investigation, we focus our attention on the electronic and pigimentary characterization of Na-free B-PAT of the *trans* form which is expected to be a potential material for practical applications. We show here that the title compound exhibits a vivid yellow color and possesses an improved solvent fastness in addition to the light and heat stability of the original compound.

EXPERIMENTAL

Equipment and Measurements

Elementary analysis was carried out for C, H, N, and S using a 2400II CHNS/O analyzer from Perkin Elmer, while the sodium content was measured by an atomic absorption spectrometer (model: SPECTRA-220FS from VARIAN). A mass spectrometer (model: AXIMA-CFR from KRATOS) was used for the analysis of Na-free B-PAT of the *trans* form. UV-visible absorption spectra in solution and in evaporated films were recorded on a UV-2400PC spectrophotometer (Shimadzu). Diffuse reflectance spectra for powders were measured on the same spectrophotometer in combination with an integrating sphere attachment (ISR-240 from Shimadzu). Reflection spectra on single crystal were measured by means of a UMSP80 microscope spectrophotometer (Carl Zeiss). A Neofluar ($\times 16$) objective was used together with a Nicol-type polarizer. Reflectivities were corrected relative to the reflection standard of silicon carbide. Diffuse-reflectance spectra were measured every 1 h in order to study the deterioration of the substance. Thermogravimetric analysis (TGA) was carried out in air for powdered Na-free B-PAT of the *trans* form using Thermo Plus TG-8120 from Rigaku.

Light stability was tested by exposing powdered Na-free B-PAT of the *trans* form to UV radiation directly under a

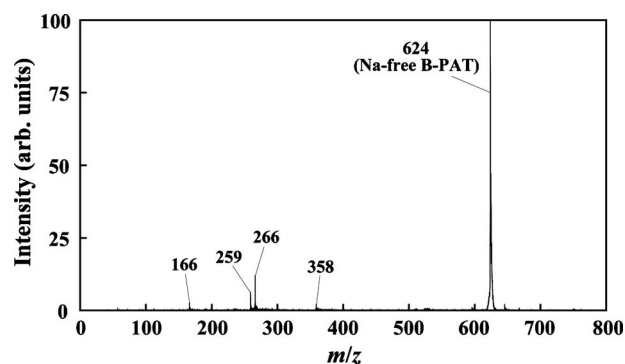


Figure 3. Mass spectrum of Na-free B-PAT of the *trans* form.

250 W ultrahigh pressure mercury lamp (USHIO) for 10 h. Solubility was measured in dimethylacetamide (DMA) and *N*-methyl-2-pyrrolidone (NMP).

Preparation and Identification of Na-Free B-PAT of the *trans* Form

The assumed B-PAT [Fig. 1(a)] (i.e., the mixture of monoazo and bisazo compounds) was synthesized in accordance with a procedure described in the patent [example 1 (0162)].² The diazonium salt was prepared by reaction of 5-amino-3-methyl-1,2,4-thiadiazole with NaNO_2 . The salt was then coupled with 4,6-bis(5-amino-3-*tert*-butyl-1*H*-pyrazole-1-yl)-1,3,5-triazine-2-ol. The elementary analysis gave the result of C: 37.17%, H: 5.10%, N: 31.97%, S: 8.34%, and Na: 2.69%. The ratio of Na-containing B-PAT to Na-free M-PAT was about 4:1 on the basis of the present analysis. Mass analysis based on the matrix-assisted laser desorption ionization gave complicated fragments, although the parent peaks for Na-containing B-PAT as well as Na-free M-PAT were clearly observed. Although B-PAT of the *cis* form [Fig. 1(a)] is uniquely claimed in the above patent,² no analytical result was presented to support this compound.

On the other hand, Na-free B-PAT of the *trans* form was prepared by addition of HCl with 30 times molar equivalent to a saturated solution in NMP of the mixture of monoazo and bisazo compounds. The product was instantaneously precipitated upon dissolution of HCl and then washed with water. Elemental analysis gave the formula of $\text{C}_{23}\text{H}_{29}\text{N}_{17}\text{OS}_2 \cdot \text{H}_2\text{O}$ which is in good agreement with the sum of the theoretical value of B-PAT (M_w : $\text{C}_{23}\text{H}_{29}\text{N}_{17}\text{OS}_2 = 623.72$) and one adsorbed water molecule. In addition, mass spectrum gave the parent peak of 624 for B-PAT together with some small fragments, as shown in Figure 3. The present B-PAT is found to be of the *trans* form as shown by the structure analysis⁶ and this is due to the fact the *trans* form is generally more stable, as also supported by our molecular orbital (MO) calculations reported in our previous paper.⁷

At this moment, it is important to note that ^1H -NMR and ^{13}C -NMR could not be used for the identification of monoazo or bisazo compounds which possess the same azo moiety because both compounds gave almost the same NMR spectra owing to the quite similar environment around the H or C atoms under consideration.

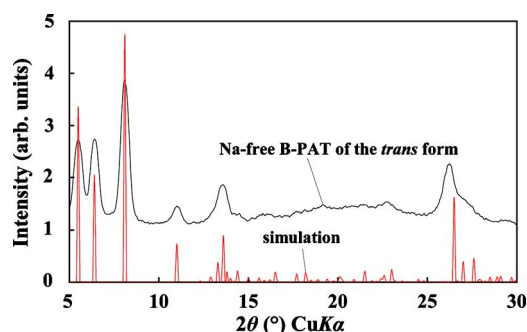


Figure 4. Powder x-ray diffraction diagram for Na-free B-PAT of the *trans* form together with the simulated diagram based on the structure analysis on single crystals.⁶

Spectroscopic Calculations on Na-Free B-PAT of the *trans* Form

Semiempirical MO calculations were carried out on Na-free B-PAT of the *trans* form using MOPAC2009.⁸ Geometry was optimized with the AM1 Hamiltonian, and the spectroscopic calculations were made on the optimized geometry using ZINDO.⁹ Although “Na-containing” B-PAT of the *cis* form should basically be calculated as the reference for Na-free B-PAT of the *trans* form, “Na-free” B-PAT of the *cis* form was instead calculated since the sodium atom is not parametrized in ZINDO.

Identification of the Powder Phase of Na-Free B-PAT of the *trans* Form

Figure 4 shows the powder x-ray diffraction diagram for Na-free B-PAT of the *trans* form together with that of the simulated diagram based on the structure analysis.⁶ The experimental diagram is in good agreement with the simulated one, indicating that the phase of single crystals is the same as that of powders.

RESULTS AND DISCUSSION

Spectroscopic Calculations

Table I shows the result of the spectroscopic calculations for Na-free B-PAT of the *trans* form, together with those for Na-free B-PAT of the *cis* form. In Na-free B-PAT of the *trans* form, the molecule is bent and each monoazo moiety gives an independent electronic transition in nearly the same wavelength region around 404 and 416 nm. In other words, each azo moiety is not linked to each other but exists independently. The former transition at 404 nm with an oscillator strength of 0.33 is a mixture of two major configuration interaction (CI) components: HOMO–1 → LUMO and HOMO → LUMO+1 (Table I), where the HOMO and LUMO denote the highest occupied or the lowest unoccupied molecular orbitals, respectively. Likewise, the latter transition at 416 nm with an oscillator strength of 1.06 has three major CI components: HOMO → LUMO+1, HOMO → LUMO+2, and HOMO–1 → LUMO (Table I). These two optical transitions give transition dipoles I and II in Fig. 1(b), respectively. However, the band at 416 nm (transition dipole II) is considered to be the major transition, as judged from the oscillator strength of the two transitions.

On the other hand, Na-containing B-PAT of the *cis* form gives only one electronic transition whose transition dipole is shown in Fig. 2(a). Here again, the transition is composed of the two CI components:

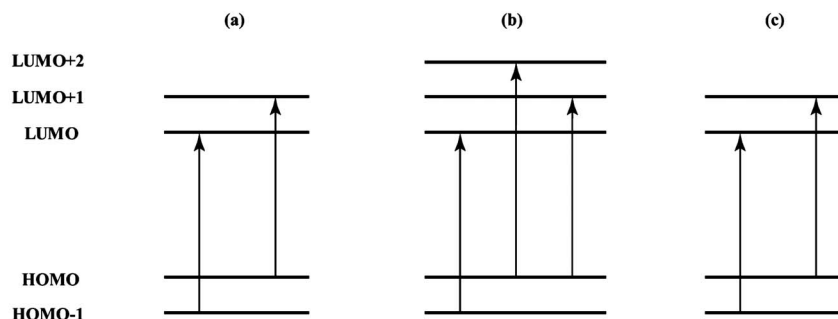
HOMO–1 → LUMO and HOMO → LUMO+1.

Solution Spectra

Figure 5 shows the solution spectrum of Na-free B-PAT of the *trans* form in NMP. The spectrum exhibits a broad band peaking at about 456 nm. The present band is a superposition of two absorption bands arising from transition dipoles I and II. If we assume that the major transition is due to transition dipole II, we can decompose the broad band to

Table I. MO calculations for Na-free B-PATS of the *trans* and *cis* forms

	λ (nm)	Osc. strength (<i>f</i>)	CI components	Transition dipole
Na-free B-PAT of the <i>trans</i> form	(a) 404.4	0.33	HOMO–1 → LUMO & HOMO → LUMO+1	Fig. 1 (b): I
	(b) 416.2	1.06	HOMO–1 → LUMO, HOMO → LUMO+2, & HOMO → LUMO+1	Fig. 1 (b): II
Na-free B-PAT of the <i>cis</i> form	(c) 411.4	1.38	HOMO–1 → LUMO & HOMO → LUMO+1	Fig. 1 (a)



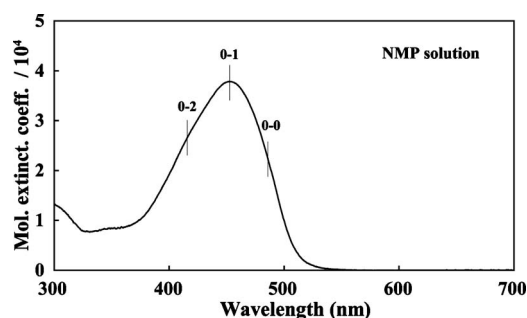


Figure 5. Solution spectrum of Na-free B-PAT of the *trans* form in NMP.

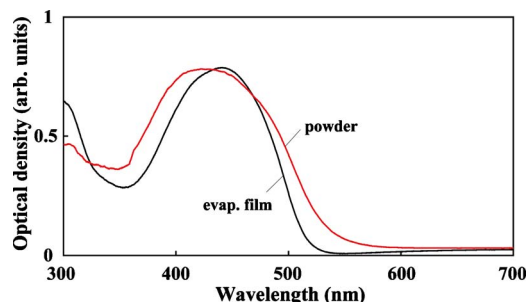


Figure 6. Diffuse-reflectance and absorption spectra of powdered and evaporated Na-free B-PAT of the *trans* form, respectively.

three vibronic transitions: the 0–0 transition (pure electronic transition) at the longest wavelength, then the 0–1 and 0–2 transitions, as shown in Fig. 5. The 0–1 or 0–2 transition is assigned to a vibronic transition of the pure electronic transition coupled with one or two vibrational transitions of about 1800 cm^{-1} , respectively.

No significant difference is observed between the spectra of Na-free B-PAT of the *trans* form and the mixture of Na-containing B-PAT of the *cis* form and M-PAT (not shown here).

Solid-State Spectra

Figure 6 shows the diffuse reflectance spectra for powdered Na-free B-PAT of the *trans* form, together with the absorption spectrum of evaporated films. The spectrum of evaporated films appreciably resembles the solution spectrum (Fig. 5). On the other hand, the diffuse reflectance spectrum is broader than that of evaporated films. In addition, the absorption maximum appears at about 420 nm which is located slightly at shorter wavelengths than that of the evaporated film. This indicates that this band can be attributed to the 0–2 transition. The evaporated film of Na-free B-PAT exhibits the typical yellow color, while the powdered Na-free B-PAT is slightly reddish.

Figure 7(a) shows the polarized reflection spectra of Na-free B-PAT of the *trans* form measured on single crystals by means of a microscope spectrophotometer. The measurement was made on the (010) plane of the crystal structure [Fig. 7(b)], where transition dipoles I and II cross each other with an angle of about 115°. Fig. 7(c) schematically illustrates the geometrical configuration of transition dipoles I and II in the unit cell [see also Fig. 1(b)]. A prominent

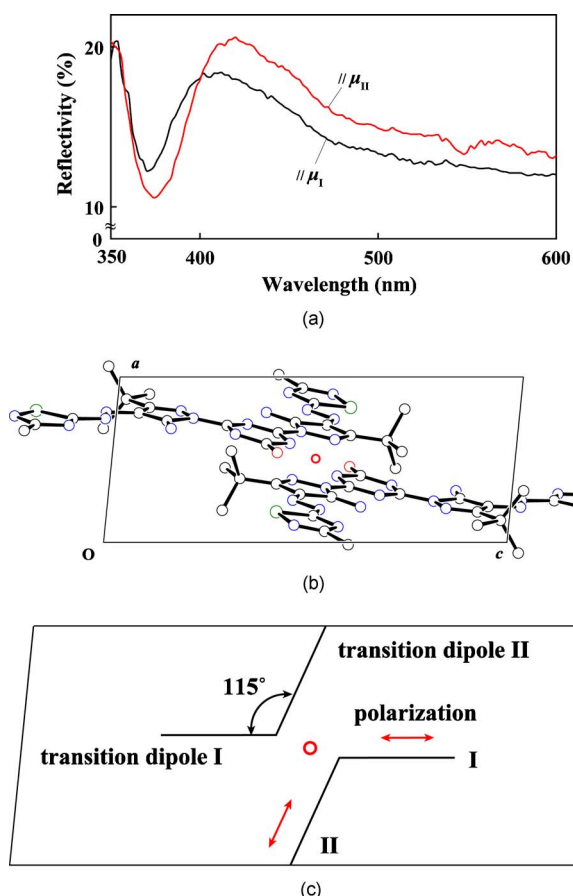
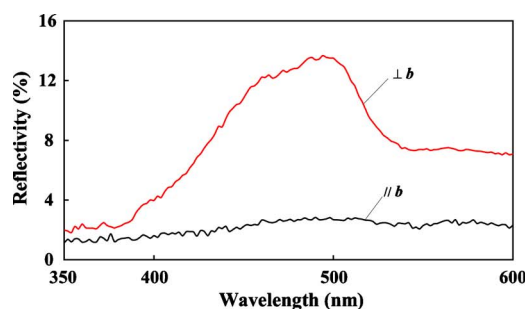


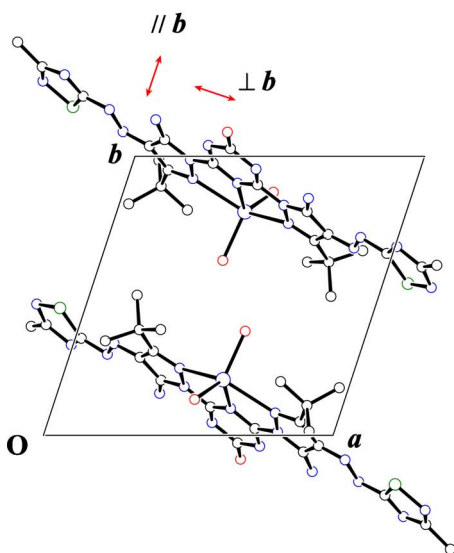
Figure 7. (a) Polarized reflection spectra measured on the (010) plane of single crystals of Na-free B-PAT of the *trans* form. (b) Projection of the structure onto the (010) plane and (c) the schematic illustration of the transition dipoles I and II, where the symbol "O" denotes the inversion center [see also Fig. 1(b)].

reflection band appears around 405 nm in Fig. 7(a) for polarization parallel to transition dipole I (i.e., nearly parallel to the *c* axis). On the other hand, a more intense reflection band is present at a longer wavelength of about 420 nm for polarization parallel to transition dipole II. In this way, we are able to separate two electronic transitions by polarized light on single crystals. The tendency of the reflection maxima and their intensity is qualitatively in good agreement with the absorption bands of MO calculations carried out for one single molecule (Table I). That is, the transition due to transition dipole I is present at a slightly shorter wavelength than that of transition dipole II, and the oscillator strength is smaller in transition dipole I than transition dipole II. The reflection maxima in single crystals can be assigned to the 0–2 transition. (Some additional remarks on the interaction between transition dipoles will be given below.)

The situation is slightly different in single crystals of Na-containing B-PAT II of the *cis* form [Fig. 2(a)], where there is only one electronic transition whose transition dipole is along the long molecular axis (Table I). Figure 8(a) shows the polarized reflection spectra of Na-containing B-PAT II of the *cis* form measured on the (001) plane of single crystals. The molecular arrangement in the (001)



(a)



(b)

Figure 8. (a) Polarized reflection spectra measured on the (001) plane of single crystals of Na-containing B-PAT II of the *cis* form and (b) projection of the structure onto the (001) plane [see also Fig. 2(a)].

plane is shown in Fig. 8(b). An intense reflection band appears around 500 nm for polarization perpendicular to the *b* axis (i.e., nearly the direction of the transition dipole). Polarization parallel to the *b* axis quenches entirely the reflection, indicating that the transition dipole points along the long molecular axis. The longest-wavelength band can be assigned to the 0–0 transition.

Interactions between Transition Dipoles

When dye or pigment molecules with high absorption coefficients are periodically arranged in the solid state, the excited state of the molecule upon light absorption travels throughout the crystal as an excitation wave: i.e., an exciton jumps from one molecule to another in the excited state. In other words, when an excitation induces a transition dipole in the molecule, the excited state in crystals involves wave functions with significant probabilities on nearest neighbors. Therefore, the exciton coupling may well involve energy contributions from interactions with all of these nearest neighbor molecules acting in concert in the lattice. This may lead to a band splitting (i.e., Davydov splitting) if the transition dipoles are arranged in an oblique fashion or to spectral displacement toward longer or shorter wavelengths if the transition dipoles are arranged in a way “head-to-tail or par-

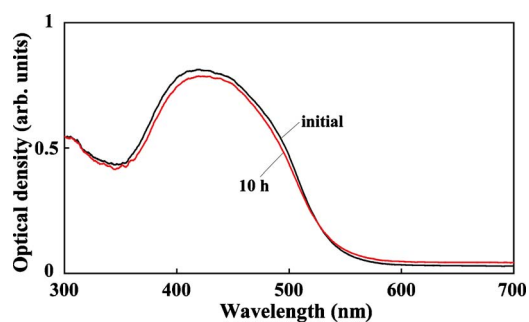


Figure 9. Diffuse reflectance spectra of Na-free B-PAT before and after UV exposure.

allel.” The interaction energy ($\Delta E_{\text{exciton}}$) is given by the dipole-dipole equation,^{10,11}

$$\Delta E_{\text{exciton}} = |\mu_T|^2 (1 - 3 \cos^2 \theta) / r^3, \quad (1)$$

where the transition dipole is denoted by μ_T and the distance and angle between two transition dipoles by r and θ , respectively. As evident from the present equation, the overall spread or shift energy is determined by the strength of the interneighbor coupling ($|\mu_T|^2$) which directly depends on the absorption coefficient of the molecule as well as the mutual relative orientation of the transition dipoles in molecular assemblies.

The above treatment is basically for molecules with one single transition moment that are arranged in a “translationally equivalent or translationally inequivalent” fashion. In our case of B-PAT of the *trans* form, the situation is slightly different because the molecule possesses two independent transition dipoles, and the molecules are arranged in a “translationally equivalent” way due to the space group of *P*-1. This means that the two kinds of transition dipoles (μ_I and μ_{II} ; see Table I) are arranged in an oblique fashion in the crystal, which leads to three kinds of excitonic interactions between μ_I and μ_I , μ_I and μ_{II} , and μ_{II} and μ_{II} . These are superimposed in the real spectrum. As judged from Table I, the oscillator strength of μ_{II} is three times larger than that of μ_I , suggesting that the μ_{II}/μ_{II} excitonic interaction is the strongest and then decreases in order of μ_I/μ_{II} and μ_I/μ_I . With all these considerations in mind, the polarized reflection spectra should basically be analyzed, but they proved rather intractable in practice, especially at the present stage of the investigation.

PIGMENTARY CHARACTERIZATION

Light Stability

Figure 9 shows the diffuse reflectance spectra of powdered Na-free B-PAT of the *trans* form before and after UV exposure. No noticeable deterioration is observed after exposure for 10 h, showing a high stability of Na-free B-PAT of the *trans* form.

Heat Stability

Figure 10 shows the TGA curve as a function of temperature for powdered Na-free B-PAT of the *trans* form. At first, a weight loss of about 3 % is observed in the temperature

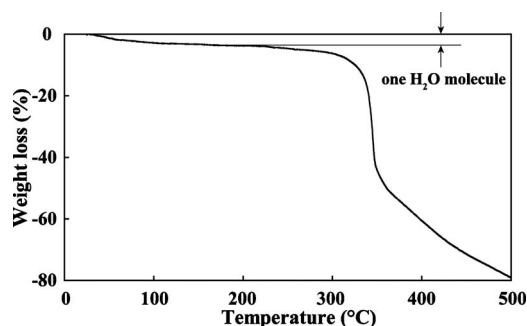


Figure 10. Thermogravimetric analysis of Na-free B-PAT of the *trans* form.

range between 50 and 250°C. This is due to the desorption of one water molecule adsorbed on the surface of Na-free B-PAT of the *trans* form, as pointed out in elementary analysis. The weight loss begins to occur abruptly around 340°C, indicating that Na-free B-PAT of the *trans* form is thermally quite stable. In addition, the abrupt weight loss is typical of one component system, as also borne out by the mass spectrum (Fig. 3). Furthermore, it is important to note that Na-free B-PAT of the *trans* form can be sublimed under high vacuum without any decomposition. This is quite unusual for ordinary bisazo compounds.

Solvent Fastness

As stated in the Introduction, the mixture of Na-containing B-PAT of the *cis* form and M-PAT exhibits a high performance in light and heat stability but is rather poor in solvent fastness. On the other hand, Na-free B-PAT of the *trans* form is found to possess much higher solvent fastness in addition to the light and heat stability.

The solubility of Na-free B-PAT in DMA and NMP is 1 and 5 g/l, respectively. This is nearly equivalent to that of Pigment Red 255 (i.e., diketopyrrolopyrrole derivative). On the other hand, Na-containing B-PAT exhibits a solubility of about 25 g/l in NMP.

CONCLUSIONS

Electronic characterization together with light, heat, and solvent fastness has been carried out on Na-free B-PAT of the *trans* form. The conclusions can be summarized as follows:

1. Na-containing B-PAT exists in the *cis* form as shown by the structure analysis and also borne out by MO calculations. However, in the absence of the sodium atom, B-PAT is found to be stabilized to the *trans* form.
2. In Na-free B-PAT of the *trans* form, there are two optical transitions in the visible region according to the MO calculations: one is the transition of 404 nm

with an oscillator strength of 0.33 composed of the two CI components: HOMO-1 → LUMO and HOMO → LUMO+1, and the other is the transition of 416 nm with an oscillator strength of 1.06 consisting of the three CI components:

HOMO → LUMO+1, HOMO → LUMO+2, and HOMO-1 → LUMO. These transitions can separately be observed by polarization on single crystals.

3. The solution spectrum of Na-free B-PAT of the *trans* form in NMP exhibits a vivid yellow color, peaking at 456 nm as characterized by a broad band between 380 and 500 nm. The absorption maximum can be assigned to the 0-1 vibronic transition. No significant difference is recognized between the spectra in solution and solid state as far as the spectral region is concerned. However, the solid state spectra are slightly broader than those in solution, and the absorption maximum is located slightly at shorter wavelengths.
4. Na-free B-PAT of the *trans* form is resistant to light, heat, and solvent. Elimination of the sodium atom from Na-containing B-PAT of the *cis* form is the key to the single component *trans* form which provides a yellow pigment that possesses good pigmentary characteristics.

REFERENCES

- ¹ M. Herbst and K. Hunger, *Industrial Organic Pigments*, 3rd ed. (VCH, Weinheim, 2004).
- ² Y. Nagata and K. Tateishi, Japan Patent 2009-73978 (2009).
- ³ H. Shibata and J. Mizuguchi, "(2,6-bis[5-amino-3-*tert*-butyl-4-[(3-methyl-1,2,4-thiadiazol-5-yl)diazenyl]-1H-pyrazol-1-yl]-4-oxo-1,4-dihydro-1,3,5-triazin-1-ido) methanol(phenol)sodium phenol tetrasolvate", *Acta Crystallogr., Sect. E: Struct. Rep. Online* **66**, m463-m464 (2010).
- ⁴ H. Shibata and J. Mizuguchi, "(2,6-bis[5-amino-3-*tert*-butyl-4-[(3-methyl-1,2,4-thiadiazol-5-yl)diazenyl]-1H-pyrazol-1-yl]-4-oxo-1,4-dihydro-1,3,5-triazin-1-ido) N-methyl-2-pyrrolidone(water)sodium N-methyl-2-pyrrolidone", *X-ray Struct. Anal. Online* **26**, 63-64 (2010).
- ⁵ H. Shibata and J. Mizuguchi, "6-[5-amino-3-*tert*-butyl-4-[(*E*)-(3-methyl-1,2,4-thiadiazol-5-yl)diazenyl]-1H-pyrazol-1-yl]-1,3,5-triazine-2,4-(1*H*,3*H*)-dione-1-methylpyrrolidin-2-one-water", *Acta Crystallogr., Sect. E: Struct. Rep. Online* **66**, o944-o945 (2010).
- ⁶ H. Shibata and J. Mizuguchi, "Crystal structure of 4,6-bis[5-amino-3-*tert*-butyl-4-[(3-methyl-1,2,4-thiazol-5-yl)diazenyl]-1H-pyrazol-1-yl]-1,3,5-triazin-2(1*H*)-one of the *trans* form", *X-ray Struct. Anal. Online* **26**, 67-68 (2010).
- ⁷ H. Shibata and J. Mizuguchi, "Four different crystals derived from a novel yellow pyrazolyl azo pigment", *J. Imaging Sci. Technol.* **55**, 020504 (2011).
- ⁸ J. P. Stewart, MOPAC2009 (Stewart Computational Chemistry, Colorado Springs, CO, 2008).
- ⁹ QUANTUM CACHE, Version 3.2 (Fujitsu, Ltd., Kanagawa, Japan, 1999).
- ¹⁰ M. Kasha, *Spectroscopy of the Excited State* (Plenum Press, New York, 1976), p. 337.
- ¹¹ D. P. Craig and S. H. Walmsley, *Excitons in Molecular Crystals* (Benjamin, Menlo Park, CA, 1968).